Random field modeling approach for uncertainty quantification of reused concrete elements

Luigi Schiano[1], Marc Fina[1], Razhan S. Ahmed[2], Oleksandr Al-Shboul[3], David Ringeloth[4], Vladislav Gudžulić[2], Stefanie Schoen[2], Jelena Bijeljic[4,5], Ernst Niederleithinger[4], Iurie Curoşu[3], Gerrit E. Neu[2], Steffen Freitag[1]

[1] *Institute for Structural Analysis, Karlsruhe Institute of Technology, 76131 Karlsruhe, Germany; luigi.schiano@kit.edu, marc.fina@kit.edu, steffen.freitag@kit.edu*

[2] *Institute for Structural Mechanics, Ruhr University Bochum, 44801 Bochum, Germany; razhan.ahmed@rub.de, vladislav.gudzulic@rub.de, stefanie.m.schoen@rub.de, gerrit.neu@rub.de*

[3] *Chair of Construction Materials, Ruhr University Bochum, 44801 Bochum, Germany; Oleksandr.Al-Shboul@rub.de, iurie.curosu@rub.de*

[4] *Division 8.2 NDT Methods for Civil Engineering, Bundesanstalt für Materialforschung und -prüfung, 12205 Berlin, Germany; david.ringeloth@bam.de, Ernst.Niederleithinger@bam.de*

[5] *University of Niš, Faculty of Civil Engineering and Architecture, 18000 Niš, Serbia; jelena.bijeljic@gaf.ni.ac.rs*

Abstract. Global sustainability goals require the reduction of waste and CO_2 emissions, motivating the reuse of reinforced concrete elements on a structural level. Assessing the structural reliability of such reused elements is particularly challenging, as their performance varies due to aging processes and exposure to environmental influences. In order to take these variabilities into account when performing structural analyses, the appropriate representation of uncertainty is crucial, see e.g. (Schoen, 2025). This contribution focuses on the generation of random fields for uncertainty quantification of spatially variable material properties of reused concrete elements, see (Botte et al., 2025). Correlation properties, such as correlation functions and lengths, are determined from measurement data (see e.g. (Fina et al., 2020)) of removed concrete elements obtained through destructive and non-destructive testing. The generated random fields are integrated into a nonlinear computational model of a reinforced concrete structure. Comprehensive probabilistic analyses are performed to show the influence of different random field approaches on the stochastic load-bearing capacity.

Keywords: Random fields, Uncertainty quantification, Reused concrete elements, Measurement data.

1. Introduction

Limited resources require a circular economy in which materials are continuously reused and recycled. Nonetheless, in structural engineering, the majority of buildings are typically still demolished, which often triggers a fatal downcycling process. However, the lack of reuse is not due to capacity deficits, but rather to utilization limits and construction regulations (Mark et al., 2025). In order to reuse structural elements, a controlled demolition process and a comprehensive assessment of their condition are required. This should be done in a fast and economical, but reliable and representative manner (Curoșu et al., 2025). Especially ensuring the reliability, which is the central task in structural design, becomes more difficult with reused elements, as geometric and material properties are not or only imprecisely known. Therefore, uncertainties have to be identified and quantified from measurements, preferably obtained from non-destructive testing, and the impact on the load bearing capacity has to be analyzed using simulation models.

Some material and geometric parameters, such as Young's modulus, strength, thickness, the position of the reinforcement, and deviations from the reference geometry (geometric imperfections), can vary spatially. Therefore, defining these parameters as uncorrelated random variables is no longer meaningful. The spatial variability of the parameters can be quantified using random fields. Structural responses, such as displacements or load-bearing capacities, can depend on the correlation properties of the random field, which are characterized by its auto-correlation function and correlation length. Several works in the literature address the definition of correlation properties. For example, (Faes et al., 2022) explore the properties of the auto-correlation function and illustrate the need for its finite differentiability. Eliáš et al. (Eliáš et al., 2015) model the material parameters of a concrete beam using auto-correlated random fields and analyze the influence of the correlation length on peak load, energy dissipation, and crack location. Lauterbach et al. (Lauterbach et al., 2018) quantitatively investigate the influence of the correlation length of random geometric imperfection fields on the stochastic buckling response of shell structures using the Karhunen-Loève Expansion (KLE). The correlation structure of the random field can be identified from experimental data, as demonstrated by Schenk et al. (Schenk and Schuëller, 2003), who employed a spectral decomposition of the covariance matrix estimated from imperfection measurements. Alternatively, Broggi and Schuëller (Broggi and Schuëller, 2011) and Papadopoulos et al. (Papadopoulos et al., 2009) use evolutionary spectra to generate random imperfections of cylindrical shells. Often, assumptions of Gaussian random fields and homogeneity are made to estimate the covariance structure. To account for the spatial non-homogeneity of geometric imperfections due to the manufacturing process, Fina et al. (Fina et al., 2026) present a non-homogeneous random field approach for the probabilistic buckling analysis of suction bucket foundations for offshore wind turbines.

A random field describes the inherent natural variability of a spatially varying quantity, i.e., the aleatory uncertainty. However, when only a limited number of measurements are available, accurately determining its correlation properties becomes challenging. This introduces an additional source of uncertainty, namely epistemic uncertainty, which results from the limited amount of available data. Consequently, both aleatory and epistemic uncertainties must be considered when characterizing the correlation structure of the random field. An overview of epistemic extensions to the aleatoric approach of random fields is given in (Schietzold et al., 2019). Dannert et al. (Dannert et al., 2021) describe extended random fields, so-called imprecise random fields, for nonlinear concrete damage analysis, where the correlation length is treated as an interval. In (Schweizer et al., 2025; Fina and Bisagni, 2026), imprecise random fields are defined to model epistemic uncertainty in shell imperfections. A fuzzy correlation model to extract correlation lengths from shell imperfection measurements, considering the limited amount of data, is introduced in (Fina et al., 2020). A sensitivity analysis of the extracted correlation length on the buckling behavior of shells is shown in (Fina et al., 2021).

In this paper, a reinforced concrete beam is investigated, which was extracted in a controlled manner from a campus building at Ruhr University Bochum. Measurements from rebound hammer testing, used as a non-destructive indicator of the compressive strength, show spatially variable material properties; see (Al-Shboul et al., 2026b). The focus of this paper lies on the estimation of correlation properties from such measurements of a reused concrete element. The random field realizations of the compressive strength are then integrated into a nonlinear computational model of the tested concrete beam. Comprehensive probabilistic analyzes are performed to demonstrate the influence of different correlation structures on the stochastic load-bearing capacity.

2. Random Fields

In this paper, variations of material parameters are modeled as correlated random fields. The basic theory is therefore briefly explained, based on (Sudret and Der Kureghian, 2000). For a given domain $\Omega \subseteq \mathbb{R}^d$ a random field $H(\mathbf{x}, \theta)$ is a collection of random variables that are assigned to each location vector $\mathbf{x} \in \Omega$ in the domain. Consequently, for a fixed $\mathbf{x}_0$, $H(\mathbf{x}_0, \theta)$ describes a random variable, with $\theta \in \Theta$ denoting the outcome, where Θ is a set of all possible outcomes. On the other hand, for a fixed outcome θ_0, $H(\mathbf{x}, \theta_0)$ describes a realization of the random field, as illustrated in Fig. 1.

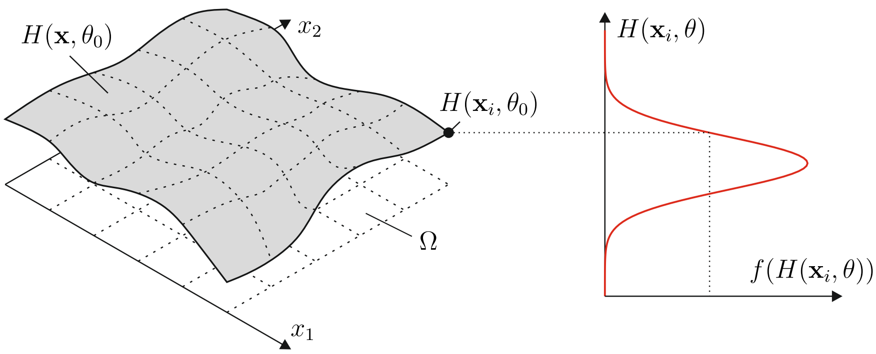

Figure 1. Realization of a random field

For the numerical implementation in a finite element model, the random field has to be discretized according to the finite element nodes. This can be done with various methods; here the so-called Karhunen-Loève expansion (KLE), see e.g. (Zhang and Ellingwood, 1994), is used. It is based on the spectral decomposition of the autocovariance function

$$C(\mathbf{x}_i, \mathbf{x}_j) = \sigma^2 \, \rho(\mathbf{x}_i, \mathbf{x}_j) \quad , \tag{1}$$

with the variance σ^2 and the autocorrelation function $\rho(\mathbf{x}_i, \mathbf{x}_j)$. The deterministic functions over which the random field is expanded then follow from the eigenvalue problem

$$\mathbf{C}\,\boldsymbol{\varphi}_i = \lambda_i\,\boldsymbol{\varphi}_i \quad \text{with} \quad \mathbf{C} = \sigma^2 \begin{bmatrix} \rho(\mathbf{x}_1, \mathbf{x}_1) & \dots & \rho(\mathbf{x}_1, \mathbf{x}_N) \\ \vdots & \ddots & \vdots \\ \rho(\mathbf{x}_N, \mathbf{x}_1) & \dots & \rho(\mathbf{x}_N, \mathbf{x}_N) \end{bmatrix} \ , \tag{2}$$

where the autocovariance matrix $\mathbf{C}$ is obtained by evaluating the autocorrelation function for every pair $(\mathbf{x}_i, \mathbf{x}_j)$ of the N finite element nodes. With the eigenvalues λ_i and eigenvectors $\boldsymbol{\varphi}_i$ the KLE can be written as

$$\hat{H}(\mathbf{x}, \theta) = \mu + \sum_{i=1}^{M} \sqrt{\lambda_i}\,\xi_i(\theta)\,\varphi_i(\mathbf{x}) \ , \tag{3}$$

where μ denotes the mean value and $\xi_i(\theta)$ a set of random variables. In the case of a Gaussian random field – that is, every vector $\{H(\mathbf{x}_1), \dots, H(\mathbf{x}_n)\}$ is gaussian – the $\xi_i(\theta)$ form a set of uncorrelated standard normal variables $\xi_i(\theta) \sim \mathcal{N}(0, 1)$. In this paper, for the autocorrelation function a quadratic exponential function is used

$$\rho(\mathbf{x}_i, \mathbf{x}_j) = \exp\left[-\frac{d(\mathbf{x}_i, \mathbf{x}_j)^2}{\ell_c^2}\right] \quad \text{with} \quad d(\mathbf{x}_i, \mathbf{x}_j) = |\mathbf{x}_i - \mathbf{x}_j| \ , \tag{4}$$

which depends only on the correlation length ℓ_c and the distance $d(\mathbf{x}_i, \mathbf{x}_j)$ of the considered finite element nodes, see Fig. 2.

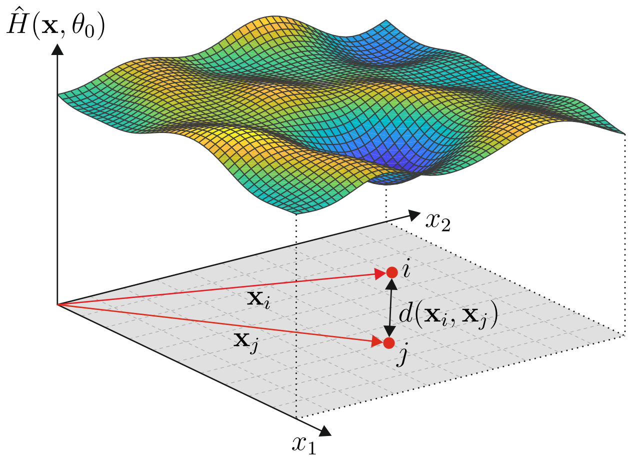

Figure 2. Realization of the Karhunen-Loêve-Expansion of a random field

The correlation length is a parameter that controls the distance in which points correlate with each other. For example, if $\ell_c \to \infty$ then all points fully correlate and every realization is a constant value. If $\ell_c \to 0$ then every point is independent and a realization of the random field is highly fluctuating. In this paper, the mean value and the variance are constant values, and the correlation function is, as already mentioned, only dependent on the distance. In this case the random field is called homogeneous.

3. Estimation of Correlation Parameters

In order to generate random fields for the uncertainty quantification of material parameters, correlation parameters such as the correlation length or the appropriate correlation function have to be determined from experimental data. In a first step, the sample mean value and variance can be estimated according to the following formulas

$$\bar{\mu}(\mathbf{x}_i) = \frac{1}{n_{smp}} \sum_{n=1}^{n_{smp}} H(\mathbf{x}_{i,n}) \ , \quad \bar{\sigma}^2(\mathbf{x}_i) = \frac{1}{n_{smp}-1} \sum_{n=1}^{n_{smp}} \left(H(\mathbf{x}_{i,n}) - \mu(\mathbf{x}_i)\right)^2 \ , \tag{5}$$

where n_{smp} denotes the number of samples. For the variance, the unbiased estimator is used, as indicated by the denominator $n_{smp} - 1$. The covariance between two random variables is defined as

$$C(\mathbf{x}_i, \mathbf{x}_j) = \mathbb{E}\left[(H(\mathbf{x}_i) - \mu(\mathbf{x}_i))(H(\mathbf{x}_j) - \mu(\mathbf{x}_j))\right] \tag{6}$$

and can be estimated analogously by

$$\bar{C}(\mathbf{x}_i, \mathbf{x}_j) = \frac{1}{n_{smp}-1} \sum_{n=1}^{n_{smp}} (H(\mathbf{x}_{i,n}) - \bar{\mu}(\mathbf{x}_i))(H(\mathbf{x}_{j,n}) - \bar{\mu}(\mathbf{x}_j))) \ . \tag{7}$$

In Fig. 3, a covariance matrix C with a quadratic exponential function and a variance $\sigma^2 = 1$ is illustrated, as well as the estimation of the covariance matrix $\bar{C}$ from 100 realizations of the KLE of the corresponding random field.

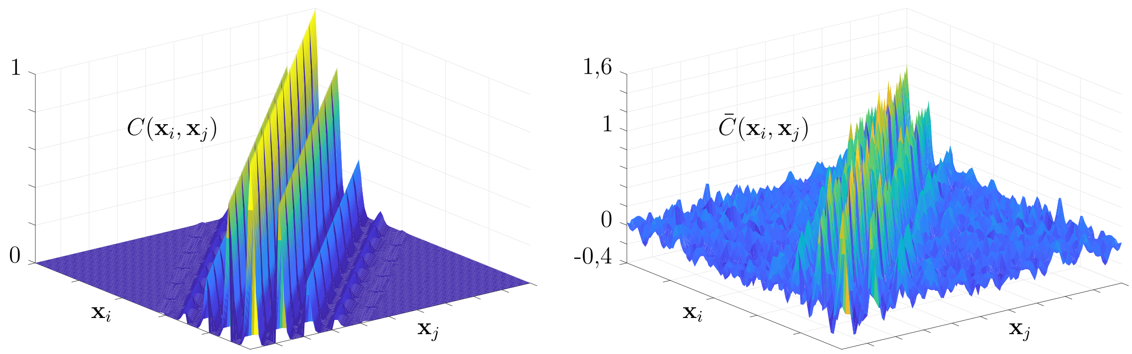

Figure 3. Covariance matrix C with quadratic exponential correlation function and variance $\sigma^2 = 1$ (left) and its estimation $\bar{C}$ from $n_{smp} = 100$ Samples (right)

Of course, the quality of the estimation directly depends on the number of samples used and according to the law of large numbers for $n_{smp} \to \infty$ it has to follow that $\bar{C} \to C$.

For the determination of the correlation length, in the next step, the autocorrelation function has to be estimated. As the goal of future work is to model the correlation length as a epistemic uncertain parameter, that is, as an interval or fuzzy variable, it has to be determined sample-wise. This can be achieved by computing the covariance matrix for each sample according to Eq. (7) and then – as the correlation function depends on the distance – sorting the covariances by the distance of the node pairs. All correlation values for one distance are finally averaged in order to obtain the correlation function for one sample. This is illustrated in Fig. 4 for one realization of a one dimensional random field with a length of 10 and a discretization with 50 nodal points.

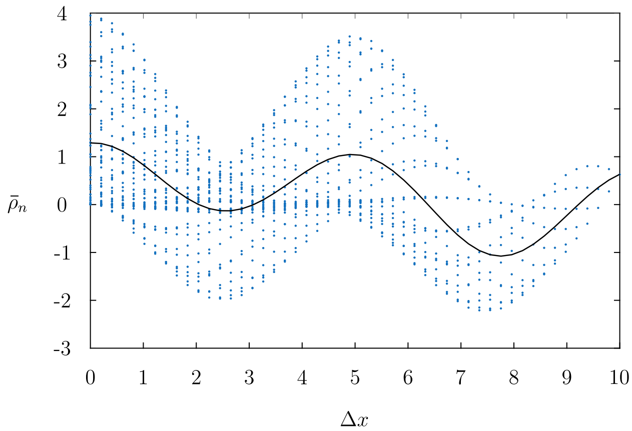

Figure 4. Correlation function $\bar{\rho}_n$ for one realization of a one dimensional random field with length of 10 and 50 nodal points, computed by averaging the correlations for each distance Δx

This approach can be expressed for the one-dimensional case with the following formula

$$\bar{\rho}_n(\xi\,\Delta x_0) = \frac{1}{N-\xi}\sum_{i=1}^{N-\xi}\frac{[H(x_{i,n}+\xi\,\Delta x_0)-\bar{\mu}(x_i+\xi\,\Delta x_0)]\,[H(x_{i,n})-\bar{\mu}(x_i)]}{\bar{\sigma}(x_i+\xi\,\Delta x_0)\,\bar{\sigma}(x_i)}\ , \tag{8}$$

where the correlation function $\bar{\rho}_n$ is calculated for every multiple ξ of the distance Δx_0. Here, all correlations for one fixed distance are directly computed and averaged. Obviously, the grid has to be uniform in this case. If the random field is two-dimensional, the correlation function can either be estimated separately for each direction or together for both directions. In the latter case, also diagonal distances are taken into account when computing the correlation function. Finally, the correlation length follows from a least squares fit with a chosen correlation function, for example the quadratic exponential correlation function defined in Eq. (4).

4. Numerical Model

In order to investigate the influence of the spatial variability of concrete properties on the structural response of reused reinforced concrete elements, a material-nonlinear finite element framework is employed. To make reliable predictions regarding the load-bearing capacity and fracture behavior, a modeling approach based on the discrete representation of cracks using zero-thickness cohesive interface elements is adopted. All material nonlinearities associated with concrete cracking under tension are described by a cohesive-frictional traction–separation relationship of the interface elements, which are inserted between the solid finite elements. Reinforcement bars are explicitly modeled using beam elements with an elastic-plastic constitutive law to account for yielding of the reinforcement. The bond-slip mechanism between the concrete and the reinforcement is represented by a bond-slip law that couples the beam element nodes to the surrounding concrete matrix according to the fib Model Code. Further details regarding the modeling approach and extensive validations can be found in (Gudžulić, 2024; Neu, 2023).

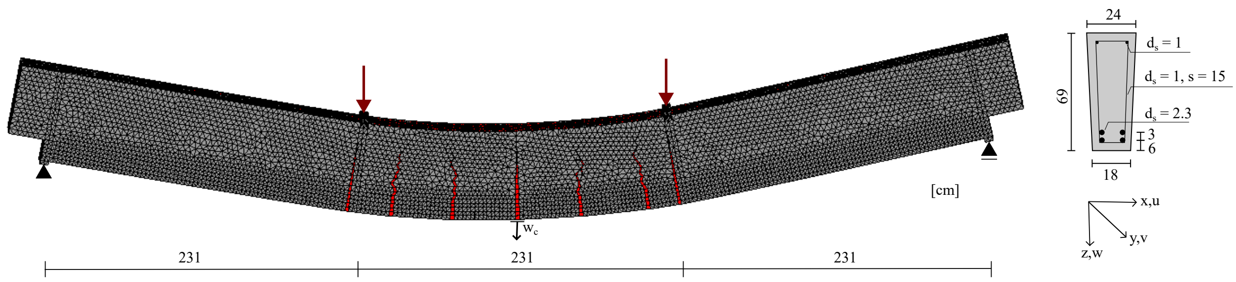

Figure 5. Numerical model of the extracted beam to predict its load-bearing capacity

The finite element model of the investigated beam is shown in Fig. 5. The beam is discretized using 177410 three-dimensional tetrahedral elements with characteristic element sizes ranging between 30 and 70 mm. The applied loading is introduced in a displacement-controlled manner to ensure a stable tracing of the structural response up to failure. The beam is supported from below at its outer edges and loaded at the quarter points in a four-point bending test.

To account for the material heterogeneity commonly observed in existing concrete structures, the concrete compressive strength is represented by a spatially correlated random field. The statistical properties of the random field are derived from the experimental measurements presented in section 5. For each realization, the random field is generated on a structured three-dimensional rectangular grid consisting of 72 072 grid points, which fully encloses the finite element model. The generated field is subsequently mapped onto the finite element mesh according to the spatial coordinates of the integration points.

Since the adopted discrete crack formulation is governed by interface properties rather than the compressive strength directly, the local compressive strength values are converted into the corresponding tensile strength and fracture energy using the empirical relationships given in Eurocode 2 (DIN, 2011) and the CEB-FIP Model Code (fib – fédération internationale du béton, 2013). The tensile strength is determined as

$$f_t = \begin{cases} 0.30\, f_c^{2/3}, & f_c \leq 50 \text{ MPa}, \\ 2.12 \ln\left(1 + \dfrac{f_c + 8}{10}\right), & f_c > 50 \text{ MPa}, \end{cases} \tag{9}$$

while the mode-I fracture energy is calculated according to

$$G_F = G_{F0}\left(\frac{f_c + 8}{10}\right)^{0.7}, \tag{10}$$

where $G_{F0} = 0.030$ N/mm corresponds to a maximum aggregate size of 16 mm. Consequently, both the tensile strength and fracture energy vary spatially according to the generated compressive strength field and directly govern crack initiation and propagation through the cohesive interface elements. In contrast, Young's modulus is kept constant for all realizations, such that the elastic stiffness and stress field remain deterministic, while the spatial variability is introduced exclusively through the fracture-related material properties.

5. Example

In the following, measurement data for the compressive strength from rebound hammer testing are analyzed. The data were obtained by the Chair of Construction Materials within the framework of the collaborative research center 1683. The broader non-destructive and destructive testing measurement campaign on the investigated elements from Ruhr University Bochum is reported in (Al-Shboul et al., 2026a). With the rebound hammer values, the surface hardness can be determined and consequently the compressive strength of the concrete can be estimated. The test was performed on several reference concrete elements, that were dismantled on the campus of Ruhr University in Bochum. In this section, data from one reinforced concrete beam with a length of 747 cm and a trapezoidal cross section with a height of 69 cm and a width of 24 cm at the top and 18 cm at the bottom (see Fig. 6), are examined regarding the generation of random fields. Fig. 6 shows a photo of the beam after cutting its edges.

Figure 6. Extracted reinforced concrete beam with cutted edges and testing areas marked in red, from (Al-Shboul et al., 2026b)

The red areas mark where the rebound hammer values were taken. Each of the 18 areas contains 11 values, resulting in a total of 198 values. Looking at the histogram of all rebound hammer values in Fig. 7, it can be seen that the data are approximately normally distributed. That is why in the following a Gaussian random field is assumed.

Although the 11 values in one area are not measured in the exact same position, they are given the same coordinate. Then, the 11 values can be treated as realizations of random variables at these locations. Furthermore, combinations of the values over all 18 spots represent realizations of

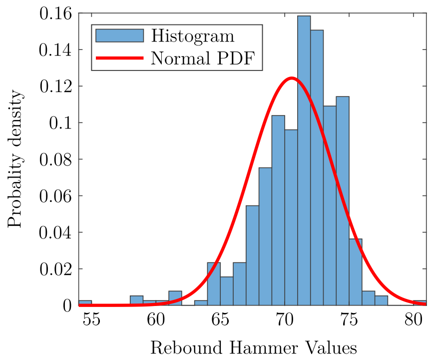

Figure 7. Histogram of rebound hammer data and fit of normal probability density function (left) and normal cumulative distribution function (right)

a random field and therefore serve as samples for the estimation of the correlation length. In total, there are 11^{18} possible combinations of all values. Out of these samples, the correlation function can be estimated and then fitted in order to obtain the correlation length. Fig. 8 shows the correlation function obtained as the mean of all correlation functions in red and the least squares fit in black. It can be seen that in the x-direction the fit closely matches the data, whereas in the z-direction the quadratic exponential function cannot exactly represent the wavy behavior of the correlation function. The determined mean values for the correlation length show, that the behavior of the random field is anisotropic, as the correlation lengths in x- and z-directions differ significantly from one another. This cannot be captured with one single correlation length in both directions and, therefore, in the following only the separate correlation lengths $\ell_{c,x}$ and $\ell_{c,z}$ are considered.

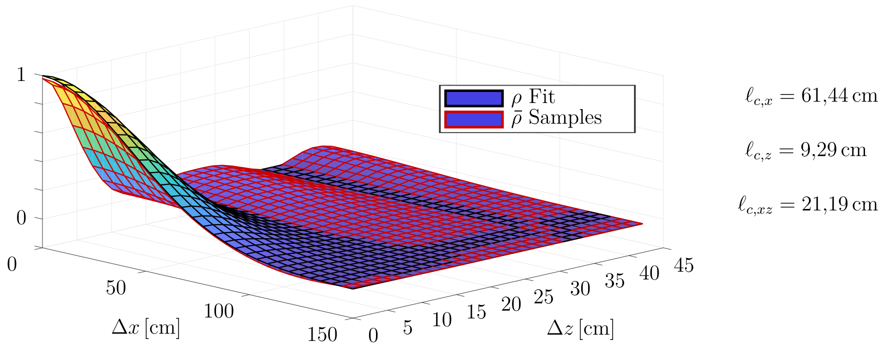

Figure 8. Mean correlation function and least squares fit for the rebound hammer measurements

Fig. 9 shows the histograms of the two correlation lengths with the minimum, maximum, and mean values. The frequency is especially high between zero and the mean value, whereas in the higher areas the values spread more and there are some outliers.

For the analysis with the numerical presented in Section 4, only the minimum, mean, and maximal values of the correlation lengths, shown in Fig. 9 are used, as the calculation is time-consuming. For the same reason, for each set of correlation lengths, only 10 realizations of the KLE of the corresponding random field are used, in order to get a first estimation of the influence of the

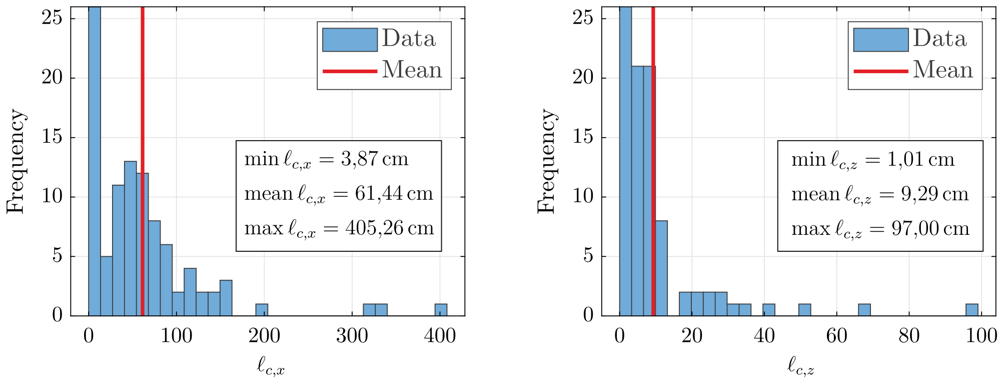

Figure 9. Histogram of the correlation lengths in x- and z-direction determined from 100 Samples

rebound hammer values on the load-bearing capacity. In total, 30 realizations of the three random fields are being computed. One realization for the mean correlation lengths $\ell_{c,x} = 61{,}44\,\mathrm{cm}$ and $\ell_{c,z} = 9{,}29\,\mathrm{cm}$ is shown in Fig. 10.

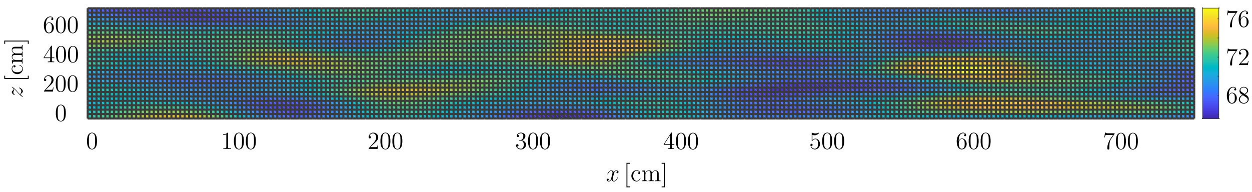

Figure 10. Realization of the KLE of the random Field of the rebound hammer values with correlation lengths $\ell_{c,x} = 61{,}44\,\mathrm{cm}$ and $\ell_{c,z} = 9{,}29\,\mathrm{cm}$

Fig. 11 presents the resulting bending moment-deflection curves of the numerical model for the three different sets of correlation lengths investigated. The colored curves represent the results from the realizations of the random fields of compressive strength. It can be seen that the random fields of the compressive strength have no significant effect on the load-bearing capacity in this investigated problem.

However, it was observed that the different random fields do have an influence on the crack pattern of the beam. This is illustrated in Fig. 12, where two crack patterns and the corresponding realizations of the random fields of the compressive strength are shown. The top one belongs to the set of minimal correlation lengths, and the bottom one corresponds to the set of maximal correlation lengths. For the realization with the maximum correlation lengths, fewer but larger cracks can be observed with a maximum crack width of 6,76 mm, whereas for the realization with the minimum correlation lengths, more but smaller cracks appear with a maximum crack width of 5,54 mm.

Further analysis on the effect of rebar corrosion in (Al-Shboul et al., 2026b) has shown that the problem is very sensitive to the rebar diameter. In the analysis the rebar diameter of the bottom longitudinal rebar was reduced from 23 to 20 mm, which should simulate corrosion of the rebar. However, it can also be interpreted as an inaccuracy in the detection of the rebar diameter. The high sensitivity indicates that the load-bearing capacity depends primarily on the rebar. The bending moment-deflection curve with rebar corrosion is also shown in Fig. 11 and has a significantly lower maximum bending moment. Therefore, in further investigations the effect of random field modeling of the rebar diameter or the tensile strength of the rebar will be examined.

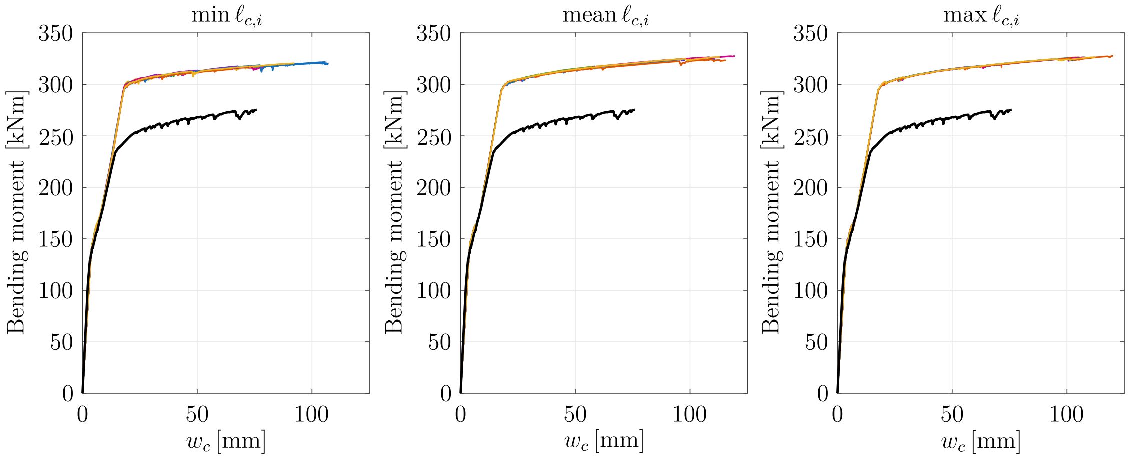

Figure 11. Bending moment-deflection curves for the three investigated sets of correlation lengths; Realizations of the random field of compressive strength are the colored curves, the effect of rebar corrosion is shown in the black curve

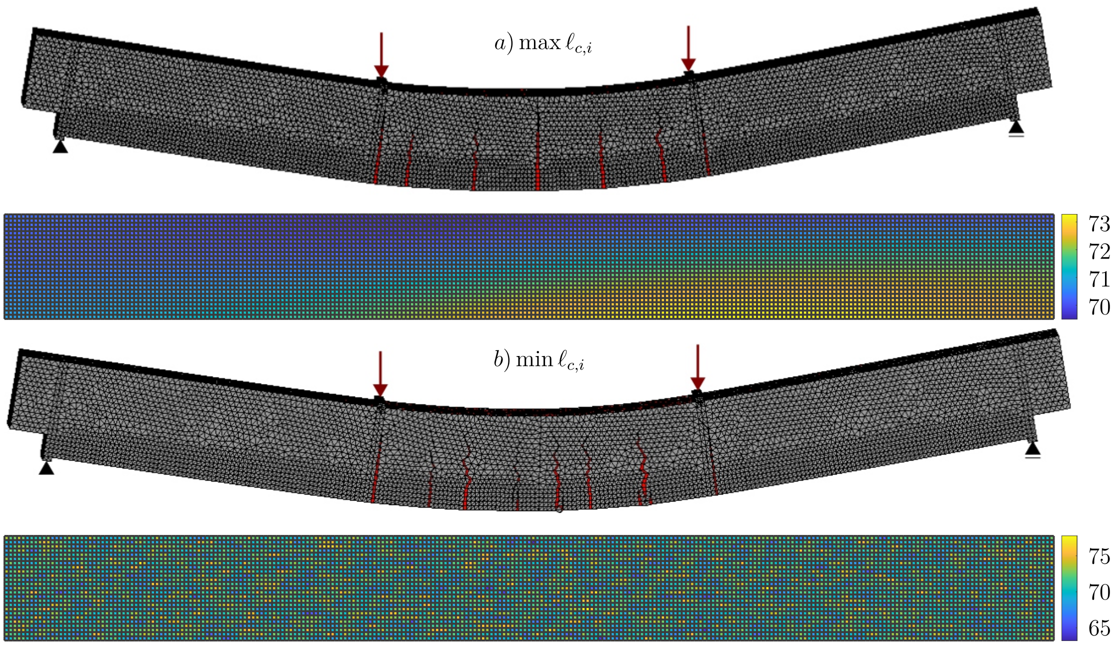

Figure 12. Crack patterns of the investigated beam and corresponding realizations of the random field of the compressive strength with a) the maximum set of correlation lengths max $\ell_{c,i}$ and b) the minimum set of correlation lengths min $\ell_{c,i}$

6. Conclusion

This study presents a way to estimate correlation parameters, such as the correlation length, out of measurement data for the modeling of material or geometric parameters as random fields. This was shown examplarily for rebound hammer measurements at an extracted reinforced concrete beam from Ruhr University Bochum. For each combination of measurements, the correlation function was determined. The correlation length for each sample was obtained by fitting the correlation function to an assumed quadratic exponential function. With the minimum, maximum and mean values of the correlation lengths, random fields were generated with the Karhunen-Loève Expansion and integrated into a nonlinear computational model of the beam. Results show that in this investigated case, the load-bearing capacity of the beam is not very sensitive to the variation of the compressive strength. In contrast, the rebar diameter to be detected has a significantly higher influence on the maximum load-bearing capacity. Therefore, in future work the influence of random field modeling of the rebar properties, such as the diameter, Young´s modulus and yield stress is investigated. Furthermore, different random field approaches, such as non-homogeneous random fields and different correlation functions will be examined.

References

Al-Shboul, O., S. Abdul-Hafiz, D. Ringeloth, N. Roumia, E. Niederleithinger, W. Z. Taffese, S. Freitag, and I. Curoşu: 2026a, 'Prediction of the Chloride Ingress Resistance of Concrete Based on Non-Destructive Tests in the Context of Structural Reuse'. *Beton- und Stahlbetonbau* pp. 1–11.

Al-Shboul, O., R. Ahmed, S. Schoen, L. Schiano, D. Ringeloth, M. Fina, J. Bijeljic, G. E. Neu, E. Niederleithinger, S. Freitag, and I. Curoșu: 2026b, 'Quantification of Spatial Variability of Concrete Parameters for the Reliability Assessment of Reused Concrete Elements'. 16th fib International PhD Symposium in Civil Engineering, accepted.

Botte, W., E. Vereecken, and R. Caspeele: 2025, 'Random Field Modelling of Spatial Variability in Concrete – a Review'. *Structure and Infrastructure Engineering* **21**(6), 1047–1060.

Broggi, M. and G. Schuëller: 2011, 'Efficient modeling of imperfections for buckling analysis of composite cylindrical shells'. *Engineering Structures* **33**(5), 1796–1806.

Curoșu, I., D. Balzani, S. Freitag, G. E. Neu, E. Niederleithinger, S. Simon, and S. Weber: 2025, 'Methoden zur Bewertung abgebauter Stahlbetonelemente für deren Wiederverwendung'. *Bautechnik* **102**(8), 483–492.

Dannert, M., M. Faes, R. Fleury, A. Fau, U. Nackenhorst, and D. Moens: 2021, 'Imprecise random field analysis for non-linear concrete damage analysis'. *Mechanical Systems and Signal Processing* **150**, 107343.

DIN: 2011, 'Eurocode 2: Design of Concrete Structures – Part 1-1: General Rules and Rules for Buildings'. DIN EN 1992-1-1:2011-01.

Eliáš, J., M. Vořechovský, J. Skoček, and Z. Bažant: 2015, 'Stochastic discrete meso-scale simulations of concrete fracture: Comparison to experimental data'. *Engineering Fracture Mechanics* **135**, 1–16.

Faes, M. G., M. Broggi, P. D. Spanos, and M. Beer: 2022, 'Elucidating appealing features of differentiable auto-correlation functions: A study on the modified exponential kernel'. *Probabilistic Engineering Mechanics* **69**, 103269.

fib – fédération internationale du béton: 2013, *fib Model Code for Concrete Structures 2010*. Berlin, Germany: Ernst & Sohn.

Fina, M. and C. Bisagni: 2026, 'Neural Network-Based Structural Optimization of Tow-Steered Composite Panels accounting for Polymorphic Uncertainty'. *Composite Structures* **387**, 120323.

Fina, M., M. Böhm, S. Freitag, P. Schaumann, and E. Ghafoori: 2026, 'Probabilistic buckling analysis of suction bucket foundations for offshore wind turbines using non-homogeneous random fields'. *Journal of Constructional Steel Research* **245**, 110531.

Fina, M., L. Panther, P. Weber, and W. Wagner: 2021, 'Shell buckling with polymorphic uncertain surface imperfections and sensitivity analysis'. *ASCE-ASME Journal of Risk and Uncertainty in Engineering Systems Part B: Mechanical Engineering* **7**(2).

Fina, M., P. Weber, and W. Wagner: 2020, 'Polymorphic Uncertainty Modeling for the Simulation of Geometric Imperfections in Probabilistic Design of Cylindrical Shells'. *Structural Safety* **82**, 101894.

Gudžulić, V.: 2024, 'Virtual Lab for Mechanical Testing of Steel and Steel-Fiber Reinforced Concrete'. Ph.D. thesis, Ruhr University Bochum.

Lauterbach, S., M. Fina, and W. Wagner: 2018, 'Influence of stochastic geometric imperfections on the load-carrying behaviour of thin-walled structures using constrained random fields'. *Computational Mechanics* **62**(5), 1107–1125.

Mark, P., D. Sanio, D. Balzani, I. Curoșu, A. Hafner, M. König, B. Kuhlenkötter, M. Thewes, W. Baille, K. Hackl, P. Hagedorn, G. Meschke, T. Nestorović, G. E. Neu, R. Sauer, M. Tafili, A. Vogel, S. Weber, M. Wichern, T. Wichtmann, E. Niederleithinger, S. Freitag, A. Menges, and S. Simon: 2025, 'Modulares Wiederverwenden von Bestandstragwerken'. *Bautechnik* **102**(8), 424–435.

Neu, G. E.: 2023, 'Computational Approaches to a Robust Segmental Lining Design in Mechanized Tunneling'. Ph.D. thesis, Ruhr University Bochum.

Papadopoulos, V., G. Stefanou, and M. Papadrakakis: 2009, 'Buckling analysis of imperfect shells with stochastic non-Gaussian material and thickness properties'. *International Journal of Solids and Structures* **46**(14), 2800–2808.

Schenk, C. and G. Schuëller: 2003, 'Buckling analysis of cylindrical shells with random geometric imperfections'. *International Journal of Non-Linear Mechanics* **38**(7), 1119–1132.

Schietzold, F., A. Schmidt, M. Dannert, A. Fau, R. Fleury, W. Graf, M. Kaliske, C. Könke, T. Lahmer, and U. Nackenhorst: 2019, 'Development of fuzzy probability based random fields for the numerical structural design'. *GAMM-Mitteilungen* **42**(1), e201900004.

Schoen, S. M.: 2025, 'Reliability Analysis and Design of RC and SFRC Structures Considering Polymorphic Uncertainties'. Ph.D. thesis, Ruhr University Bochum.

Schweizer, M., M. Fina, W. Wagner, and S. Freitag: 2025, 'Optimization of shell structures with fuzzy probability-based random fields using artificial neural networks'. *Proceedings in Applied Mathematics and Mechanics (PAMM)* **25**(4), e70038.

Sudret, B. and A. Der Kureghian: 2000, 'Stochastic Finite Element Methods and Reliability A State-of-the-Art Report'. Technical report, Department of Civil & Environmental Engineering, University of California, Berkeley.

Zhang, J. and B. Ellingwood: 1994, 'Orthogonal Series Expansions of Random Fields in Reliability Analysis'. *Journal of Engineering Mechanics* **120**(12), 2660–2677.